



# Mapping nectar-rich pollinator floral resources using airborne multispectral imagery

S.L. Barnsley<sup>a,\*</sup>, A.A. Lovett<sup>b</sup>, L.V. Dicks<sup>c,a</sup>

<sup>a</sup> School of Biological Sciences, University of East Anglia, Norwich Research Park, Norwich, Norfolk, NR4 7TJ, UK

<sup>b</sup> School of Environmental Sciences, University of East Anglia, Norwich Research Park, Norwich, Norfolk, NR4 7TJ, UK

<sup>c</sup> Department of Zoology, University of Cambridge, Cambridge, CB2 3EJ, UK

## ARTICLE INFO

### Keywords:

Pollinator  
Mapping  
Sub-meter  
Agri-environment  
Maximum likelihood

## ABSTRACT

Wild pollinator numbers are known to be positively associated with amounts of flower-rich habitat at landscape level. Increasing floral resources can be particularly beneficial in relatively nectar-poor agricultural systems and having a baseline understanding of the temporal and spatial availability of resources can allow targeted habitat management. Very high-resolution remote sensing has potential to facilitate accurate mapping of fine-scale, within-habitat pollinator foraging resources, thereby allowing spatial and temporal gaps to be identified and addressed, improving predictions of pollinator numbers, and enabling remote monitoring of pollinator conservation measures.

Concentrating on hedgerow and flower-rich field margins in a UK agricultural landscape, we showed that multispectral airborne imagery with 3 cm and 7 cm spatial resolutions can be used to classify five nectar-rich flowering plant species (*Prunus spinosa*, *Crataegus monogyna*, *Rubus fruticosus*, *Silene dioica* and *Centaurea nigra*) using a maximum likelihood classification algorithm. In 2019, we separately acquired 3 cm and 7 cm imagery for the months of March, May and July, respectively. Overall accuracies were above 90% for each month at both 3 cm and 7 cm resolutions (range 92.32%–98.72%), supporting previous research that suggests higher spatial resolutions do not necessarily lead to higher accuracies, as pixel variability is increased.

Remaining challenges include determining which co-flowering species of similar colours in the visible range can be distinguished from one another within classifications and quantifying floral unit density from classifications so that the nectar sugar supply can be calculated. Nonetheless, we provided a prototype approach for mapping pollinator foraging resources in an agricultural context, which can be extended to other nectar-rich species. The foundation is set for developing a remote sensing pipeline that can provide valuable data on the availability of nectar-rich flowering plant species at different time-points throughout the year.

## 1. Introduction

### 1.1. Meeting pollinator resource requirements

Land-use changes linked to the intensification of agricultural activities are key contributors to pollinator decline (Dicks et al., 2021; Goulson et al., 2015; Ollerton, 2017; Potts et al., 2010, 2016). In the UK for example, Ollerton et al. (2014) found that increased extinction rates for wasps and bees coincided with shifts in agricultural policy, such as agricultural intensification following the First World War. Baude et al. (2016) discovered that pollinator decline patterns in Britain mirrored reductions in nectar supply and diversity. This and other studies (e.g.

Carvell et al., 2017; Pywell et al., 2005; Scheper et al., 2013) suggest that increasing the availability and variety of nectar-rich flowering plant species could go a long way in addressing pollinator losses.

Arable habitat produces the least nectar out of all of Britain's habitat types as well as the least variety (Baude et al., 2016). Increasing and better managing existing pollinator foraging resources alongside crops could therefore contribute greatly to conservation efforts.

Positive relationships have long been established between broad landscape level vegetation categories and pollinator or crop-visitor metrics, such as species richness and abundance (Pywell et al., 2005; Scheper et al., 2013; Willcox et al., 2018; Kleijn et al., 2015; Ricketts et al., 2008). However, knowledge surrounding the specific

\* Corresponding author.

E-mail address: [sarah.barnsley@bluewin.ch](mailto:sarah.barnsley@bluewin.ch) (S.L. Barnsley).

<https://doi.org/10.1016/j.jenvman.2022.114942>

Received 8 October 2021; Received in revised form 28 February 2022; Accepted 18 March 2022

Available online 11 April 2022

0301-4797/© 2022 The Authors. Published by Elsevier Ltd. This is an open access article under the CC BY license (<http://creativecommons.org/licenses/by/4.0/>).

within-habitat variables contributing to these relationships, such as availability of nesting sites or nectar/pollen supply, remains limited (Willcox et al., 2018). Some studies do address these relationships, such as Holl (1995), who demonstrated that butterfly species richness and abundance both increased with greater nectar sugar supply (grams), at reclaimed sites previously surface-mined for coal. Timberlake et al. (2021) found that *Bombus terrestris* colony density increased as the farm-level nectar sugar supply ( $\text{g}/\text{m}^2/\text{day}$ ) in September increased.

Precise estimates of how resources such as pollen and nectar vary temporally and at different spatial scales are essential for understanding the numbers of pollinators that can be supported at a habitat or landscape level, and for quantifying resource shortfalls (Carl et al., 2017; Jachuta et al., 2021; Langlois et al., 2020; Timberlake et al., 2019). Jachuta et al. (2021) for example, found that nectar sugar supply ( $\text{kg}/\text{km}^2$ ) did not meet honeybee sugar demand in March or June, or bumblebee sugar demand in June, in Polish upland landscapes. Similarly in the UK, Timberlake et al. (2019) showed that farm-level nectar sugar supply ( $\text{g}/\text{km}^2/\text{day}$ ) did not meet bumblebee sugar demand in March, June or late summer.

A baseline map detailing the spatial and temporal distribution of floral resources such as nectar and pollen, would allow any gaps to be identified and addressed through the selection of appropriate interventions. For example, a greater nectar sugar supply in spring could be encouraged by increasing the floral abundance of nectar-rich hedgerow species such as *Prunus spinosa* or *Crataegus monogyna*, which flower at that time of year. Staley et al. (2012) demonstrated that *Crataegus monogyna* flower abundance could be increased by more than two-fold by cutting hedgerows every 3 years as opposed to annually. Alternatively, flowering plant species that provide nectar/pollen resources during temporal resource gaps could be included in sown wildflower strip/margin mixes (Nowakowski and Pywell, 2016) and additional wildflower strips could be created where spatial gaps between resources are greater than pollinator foraging distances (Greenleaf et al., 2007).

However, field surveying of floral resources to gather baseline distribution information at finer scales is usually time and space limited. Often, only a subset of floral resources can be mapped and subsequently used to estimate resources available at the wider habitat or landscape level (e.g. Baude et al., 2016; Pettorelli et al., 2018; Timberlake et al., 2019). Remote sensing has enormous potential to facilitate the fine-detailed mapping of pollinator resources and fill in research gaps (e.g. see Galbraith et al., 2015; Willcox et al., 2018).

### 1.2. Remote sensing for mapping pollinator resources

Pollinator researchers have started taking advantage of remote sensing opportunities (Galbraith et al., 2015; Gardner et al., 2020; Willcox et al., 2018). Carrié et al. (2018) used multispectral satellite imagery with a 2 m pixel size to determine the relationship between nesting resource metrics in permanent grassland habitats and the bee communities in crop fields. Xavier et al. (2018) developed a technique using Unmanned Aerial Vehicle (UAV) imagery with a pixel resolution of 1 cm to capture the floral resource within experimental plots. They produced classification outputs with three categories: bare ground, flowers and other vegetation. Pollinator visits were found to positively correlate both with field survey flower counts and floral area as obtained from these classification outputs ( $p$ -values of  $<0.001$  and  $0.0007$ , respectively).

While not focusing specifically on pollinator ecology, Bradter et al. (2020) used airborne hyperspectral imagery and simulated multispectral data with a 1 m pixel resolution, to classify farmland grassland habitats into distinct vegetation categories. Vegetation categories were grouped according to dominant plant species or British National Vegetation classification categories. There remain very few studies globally that focus specifically on mapping floral resources (Landmann et al., 2018). However, a few studies have demonstrated that flowers of

individual plant species growing in stands with relatively little diversity can be detected using remote sensing, for example when monitoring invasive species (e.g. Carl et al., 2017) or fruit crops (e.g. Horton et al., 2017). Carl et al. (2017) achieved an overall accuracy of 99.5% when using ImageJ to distinguish between invasive *Robinia pseudoacacia* L. flower and vegetation biomass pixels in red-green-blue UAV imagery. Horton et al. (2017) created a peach blossom detection algorithm in MATLAB which they used to detect peach blossom pixels with an 84.3% success rate using multispectral UAV imagery. Chen et al. (2009) demonstrated that hyperspectral data acquired with a spectroradiometer could be used to estimate the floral cover of *Halerpestes tricuspis* in a Tibetan grassland context in July, when this species was the dominant flowering species. Dixon et al. (2021) demonstrated that a maximum likelihood classifier could be used to classify *Corymbia calophylla* flower pixels with a 2 cm spatial resolution with user's and producer's accuracies ranging between 89.9%–92.9% and 89.8%–96.4%, respectively.

These studies demonstrate potential for high-resolution remote-sensing technology to create baseline maps of key pollinator foraging resources across entire farmed landscapes, including small-scale flowering plants in field margins, such as *Centaurea nigra* and *Leucanthemum vulgare* (Baude et al., 2016). Quantifying the floral cover of individual flowering plant species is important because they differ widely in their provision of nectar and pollen (Baude et al., 2016). For example, for those UK species with empirical nectar data available, flow rates per flower vary by three orders of magnitude, ranging from 0 to 7667.84  $\mu\text{g}$  sucrose/flower/day (Baude et al., 2015a). Flowering plant species also differ in their ability to provide floral resources to different pollinator species or functional groups (e.g. Dicks et al., 2015, Table S1). None of the aforementioned studies determined whether the floral unit cover of individual flowering plant species within arable field margins can be accurately classified and mapped using very high spatial resolution remotely sensed data. Throughout this study we have used the definition of Carvell et al. (2007) for floral units: either individual flowers or stems with multiple flowers that a bee can walk rather than fly between, e.g. one *Centaurea nigra* capitulum.

Flowering hedgerow species also provide an important food resource to pollinators in farmed landscapes (Baude et al., 2016; Garratt et al., 2017; Häussler et al., 2017; Timberlake et al., 2019). While hedgerow locations in a landscape have been successfully mapped (Betbeder et al., 2015; Tansey et al., 2009; Vannier and Hubert-Moy, 2008; Vannier et al., 2011), to our knowledge, flowering plant species and the extent of their floral cover in a northern European hedgerow context have not.

In this study we focus on mapping nectar-rich flowering plant species found within UK agricultural field margins and hedgerows, because of the high potential value of these habitat types for pollinators (Baude et al., 2016; Timberlake et al., 2019; Häussler et al., 2017). We focus on nectar-rich species as a starting point, as nectar sugar constitutes a key energy source for pollinators (Willmer, 2011). We determine whether the floral unit cover of three nectar-rich hedgerow species (*Prunus spinosa*, *Crataegus monogyna* and *Rubus fruticosus*) and two arable margin species (*Silene dioica* and *Centaurea nigra*) can be classified and mapped using multispectral airborne imagery and a maximum likelihood (ML) classifier.

In addition to identifying spatial and temporal gaps in nectar-rich floral resources to inform on-farm conservation, remotely-sensed maps of nectar resources could feed into spatially explicit models. Such models have been developed to predict pollinator abundance or provision of pollination services, according to landscape structure (e.g. Lonsdorf et al., 2009; Gardner et al., 2020). Most such models rely on estimates of floral and nesting resources for a particular land cover category/habitat type, derived from expert opinion, evidence in the scientific literature or scaled up from field data acquired from a subset of a study area. Remotely-sensed maps that precisely outline the fine-scale floral cover distribution of flowering plant species across an entire study area could potentially increase the accuracy of spatially-explicit models,

although this will need to be tested empirically.

### 1.3. Choice of classifier and spatial resolution

In this study, we chose to use an ML classifier because we were working in collaboration with an industry partner H L Hutchinsons Ltd. (Hutchinsons, 2021), who was interested in developing a remote sensing method that could be used relatively cheaply and easily on the ground. The ML classifier meets these requirements and is readily available through multiple software packages (Lu and Weng, 2007). This parametric classification approach relies on the distribution of pixel values within data bands. Based on this distribution, the ML classifier then allocates each pixel to the classification category that it is most likely to belong to (Lillesand et al., 2015). More recently, much remote sensing research has turned to machine-learning classifiers such as random forest. However, at the time of our research most software packages that offered random forest either had a substantial cost involved (e.g. eCognition) or required a detailed knowledge of coding (e.g. the ‘randomForest’ package in R) rather than an easy to use graphical-user-interface (Belgiu and Drăguț, 2016). The latter would make random forest an impractical classifier for use within routine agricultural operations. ML classification algorithms have been successfully used for many ecological remote sensing applications, such as mapping wetlands (Guo et al., 2017) or producing maps of land use/land cover change (Islam et al., 2018).

Choice of imagery spatial resolution was another important consideration for this study. Too high a spatial resolution can lead to greater within-class spectral variability and a greater chance of spectral signature overlap between differing features (Pu et al., 2011; Gong and Howarth, 1990; Latty et al., 1985; Toll, 1985). On the other hand, too low a spatial resolution in the context of individual floral units could lead to a greater chance of mixed pixels which could result in reduced classification accuracies for individual flowering plant species (Foody and Arora, 1996; Shanmugam et al., 2006). As the floral unit width of our flowering plant species of interest ranged between 1 and 3 cm (NatureGate, 2020), we chose a pixel width of 3 cm as a starting point. However, the standard pixel size used by many farmers for crop monitoring in the UK is 7 cm. As a 7 cm spatial resolution is widely used and considerably cheaper than a 3 cm resolution, we also investigated whether a 7 cm pixel size could classify our flowering plant species of interest.

Specifically, we addressed the following research question:

Can multispectral airborne imagery with spatial resolutions of 3 cm and 7 cm be used to accurately classify the floral unit cover ( $m^2$ ) of nectar-rich flowering plant species in hedgerow and wildflower margins, as determined through overall, user’s and producer’s accuracy metrics and F-scores?

## 2. Methods

### 2.1. Study site and target nectar-rich flowering plant species

Our study site was located within a conventional arable farm in Northamptonshire, approximately 76 miles to the north-west of London, UK (52°17’57”N, 0°45’49”W). The farm was 809ha in size and the predominant crops were wheat, barley and oilseed rape. One field was used as our study site (Fig. 1). Two sides of the field were sown with margins that had been planted with a pollinator wildflower mix from a UK-based wildflower seed provider: Emorsgate seeds (Emorsgate Seeds, 2021; see Supporting Table 1). The full list of species included as part of the mix can be found in Supplementary Data 1. Some species not included in the mix were also growing in the margins, such as *Trifolium repens*. The field was surrounded on two sides by hedgerow containing *Prunus spinosa* and *Crataegus monogyna* and on a third side by thick *Rubus fruticosus* scrub.

When deciding on our target margin flowering plant species, these

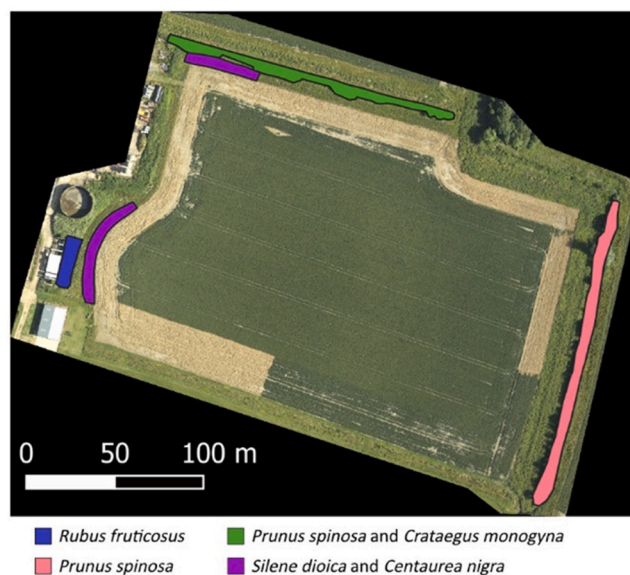


Fig. 1. The study field with the areas used for selecting training and verification pixels for each flowering plant species highlighted.

had to be distributed across several margin subsections and flowering abundantly enough within our margins to provide adequate ground-truth data for the classification stage. Following Fisher et al. (2018), we considered a minimum of 100 pixels adequate for training and verifying a classification (see Section 2.3 for further detail). Of the flowering plant species that met this criterion, for each image acquisition date (28th March, 14th/15th May and 4th July) we selected the species within the wildflower mix that produced the greatest quantity of nectar per floral unit (floral units defined in Section 1.2) according to data from Baude et al. (2015a) and Baude et al. (2015b). We selected *Silene dioica* as our target margin flowering plant species for May and *Centaurea nigra* as our target flowering plant species for July (See Table 1). No margin species were flowering in March.

There were fewer nectar-rich flowering plant species within hedgerows. Subsequently, hedgerow species were included as target species in our study if they were flowering abundantly enough to generate adequate ground-truth data for the classification stage (i.e. at least 100 pixels of data covering several hedgerow subsections or a hedgerow section of greater than 3 m). Our target species were *Prunus spinosa* flowering in March, *Crataegus monogyna* flowering in May and *Rubus fruticosus* flowering in July (Table 1).

### 2.2. Acquisition and processing of aerial imagery

Remotely sensed aerial imagery was acquired from March–July 2019 by Spectrum Aviation, using two Hasselblad A6D-100c (50 mm) cameras attached with bayer filters. Two sets of data with spatial resolutions of approximately 3 cm and 7 cm were obtained for each month. Imagery was acquired on 28th March (3 cm and 7 cm data – acquired consecutively), 14th May (7 cm data), 15th May (3 cm data) and 4th July (3 cm and 7 cm data – acquired consecutively). The sensors were mounted on a Sky Arrow 650 manned aircraft. Data acquisition flights were only launched on days that were forecast to be cloud-free (no more than 1/8 cloud coverage, with visibility greater than 10 km) and with low wind (<20 kts).

Spectrum Aviation carried out the initial pre-processing. Agisoft Metashape (Agisoft, 2019) was used to tie the images together. Data were processed under a WGS 84 (EPSG: 4326) coordinate reference system (CRS). However, the final 6-band orthomosaics for each month and resolution were exported for use within classifications under an

**Table 1**

Target nectar-rich flowering plant species for which field data were gathered, their nectar production values and approximate floral unit size.

Date of image acquisition	Dates gathered ground-truth data	Location (margin/hedgerow)	Flowering plant species (common name)	Nectar sucrose secretion rate per floral unit per day ( $\mu\text{g}$ ) <sup>a</sup>	Approximate floral unit <sup>b</sup> width (cm)
28 March	NA	Hedgerow	<i>Prunus spinosa</i> (blackthorn)	266.23	1.0–1.8 <sup>c</sup>
14/15 May	NA	Hedgerow	<i>Crataegus monogyna</i> (hawthorn)	102.47	1.0 <sup>c</sup>
14/15 May	15–18 May	Margin	<i>Silene dioica</i> (red campion)	450.65	2.0–3.0 <sup>c</sup>
4 July	04–11 July	Margin	<i>Centaurea nigra</i> (common knapweed)	10,705.66	2.4 (0.9) <sup>d</sup>
4 July	NA	Hedgerow	<i>Rubus fruticosus</i> (bramble)	1892.83	1.9 (0.1) <sup>d</sup>

<sup>a</sup> Mean nectar sucrose per flower from Baude et al. (2015a) multiplied by mean no. flowers per floral unit from Baude et al. (2015b).

<sup>b</sup> Note that the term floral 'unit' in the table uses the definition of Carvell et al. (2007) whereby any flower or stem with multiple flowers that a bee can walk rather than fly between constitutes one unit.

<sup>c</sup> Values from NatureGate (2020) and only an approximate value.

<sup>d</sup> The values for *Centaurea nigra* (n = 11) and *Rubus fruticosus* (n = 10) are means from our own measurements obtained in 2020 (see Supporting Data 1). Variance is reported in the brackets.

OSGB 1936/British National Grid (EPSG: 27700) CRS.

We imported the final 6-band 16 bit orthomosaic images for each month into QGIS version 3.4.15 (QGIS, 2020) and split the stacked images into their component bands. Three of the six bands were acquired using a dual filter. They each contained a combination of red and near-infrared (NIR) wavelengths and only the one which had the highest proportion of NIR was kept, along with the red-green-blue (RGB) bands. Each band was 15 nm wide.

The RGB and NIR bands were stacked back together into a 4-band image for each month which was used in the classification process. As we were interested in whether aerial imagery could accurately map high nectar-producing floral resources at a single point in time, we did not convert from digital number values to reflectance, following Xavier et al. (2018).

### 2.3. Gathering ground-truth data for margin species

We collected ground-truth data within eight days of each image acquisition date (Table 1). For our margin species, ground-truth data were gathered for individual remote sensing (RS) units. For *Centaurea nigra*, RS units were defined in the same way as floral units following Carvell et al. (2007), i.e. one capitulum constituted an RS unit (Fig. 2a). Such an approach was not possible for *Silene dioica* because for this species floral units as defined by Carvell et al. (2007) are individual flowers. For remote sensing purposes, any *S. dioica* flowers on the same main stalk were counted as a single RS unit, because they would be likely to occur within the same pixel space in the aerial images (Fig. 2b and c).

Location data were gathered for 85 *S. dioica* RS units and 100 *C. nigra* RS units. RS units for each species were purposively selected based on how they were spread across the margins (See Supporting Methods 1).

Two techniques were used to accurately measure the location of individual RS units. Distances to at least two ground-control points

(GCPs) were measured on the ground using a DeWALT laser beam measure ( $\pm 1.5$  mm) (see Xavier et al., 2018; see Supporting Methods 2). In addition, for a subset of RS units we gathered waypoint locations using a Topcon Real-time Kinetic (RTK) HiPer V receiver (Topcon, 2020).

### 2.4. Locating flowering plant species within the imagery

We tested the accuracy of the RTK receiver by recording waypoints at the corners of a ground-control point board. As the waypoints were not located in the correct position in the imagery, we found the RTK receiver to be an inaccurate means of locating *Silene dioica* and *Centaurea nigra* RS units in May and July imagery, respectively. This could have been due to error e.g. multipath error which is caused when the path of a signal between RTK receiver and satellite is altered due to reflection off a nearby feature (Kos et al., 2010; Mekik and Can, 2010). We subsequently only used RS unit location data obtained via our method of measuring the distance of RS units to known ground-control points (GCPs).

Even when measuring the distance of RS units to known GCPs, there was no way of determining exactly what error was involved in the ground location measurements relative to the imagery. For example, gusts of wind could change RS unit locations at the exact moment that an image was acquired. We were consequently unable to precisely locate individual RS units within the imagery. However, we had gathered data for multiple RS units within clusters of floral units of *S. dioica* and *C. nigra* (Supporting Methods 1). We also knew that non-target flowering plant species with potentially similar spectral signatures in the visible range were either not flowering synchronously with *S. dioica* or *C. nigra*, or were located in different parts of the margin. For example, *Cirsium arvense* was flowering synchronously to *C. nigra*, but *C. arvense* floral units were at the very least several metres away from the *C. nigra* RS units that were used in the ground-truth process. We therefore combined

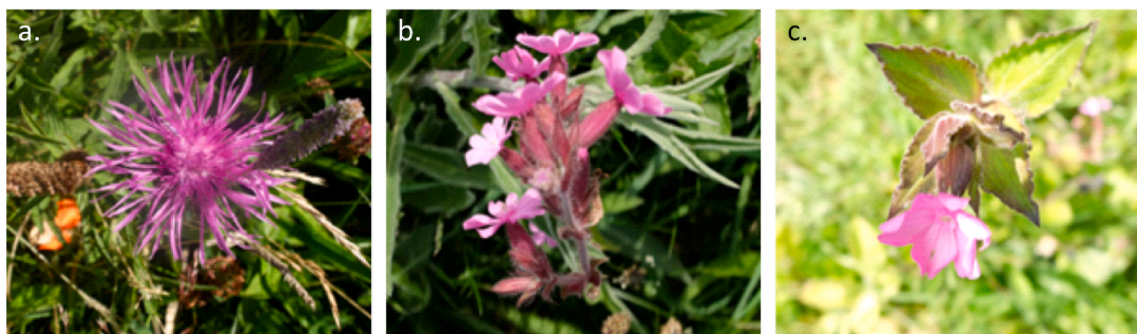


**Fig. 2.** a. One *Centaurea nigra* capitulum constitutes a remote sensing unit. b. One *Silene dioica* remote sensing unit with multiple flowers. c. A second *S. dioica* remote sensing unit with only one flower.

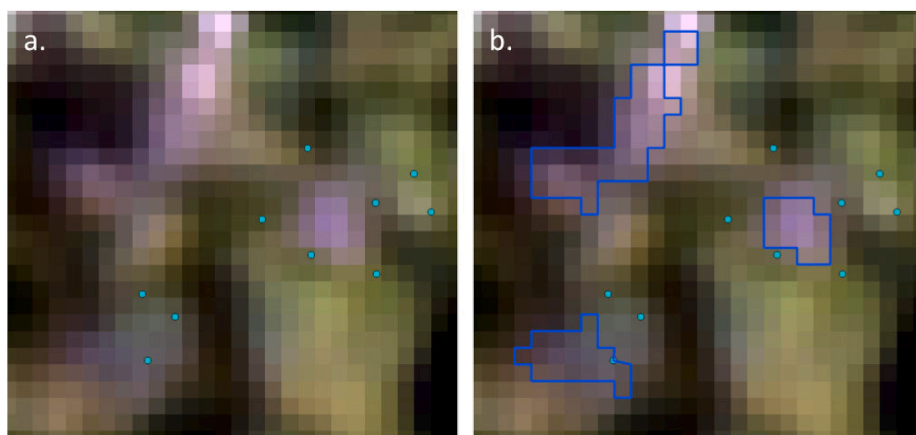


**Fig. 3.** a. Measured locations of individual *Centaurea nigra* remote sensing (RS) units within 3 cm imagery (pale blue points). These multiple RS unit locations outline an area of flowering *C. nigra* which given our knowledge of the surrounding margin area, meant we assumed purple pixels within close proximity (within 0.60 m) to the predicted RS unit locations belonged to *C. nigra*. There is no certainty that each point falls exactly on top of an RS unit in the image. b. The same image with *C. nigra* training pixels outlined. (For interpretation of the references to colour in this figure legend, the reader is referred to the Web version of this article.)

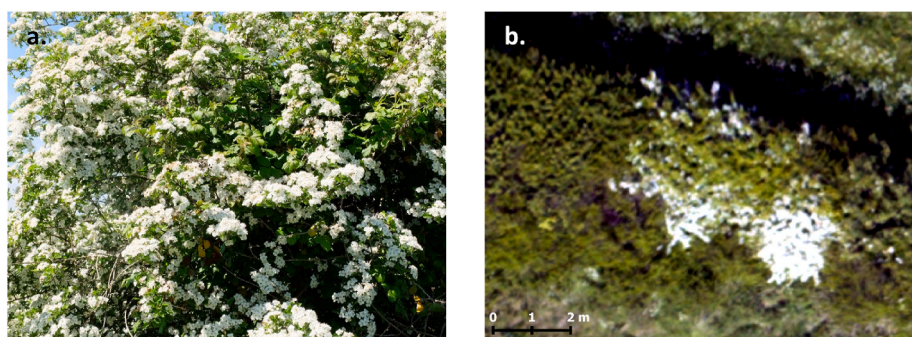


**Fig. 4.** a. An image of a patch of *Crataegus monogyna* taken from the ground. b. A sub-section of the multispectral image for May (3 cm resolution) showing a patch of flowering *Crataegus monogyna*.

the ground-truth data (RS unit locations - 85 for *S. dioica* and 100 for *C. nigra*) and knowledge of the surrounding area with the fact that *S. dioica* and *C. nigra* are both distinct pink/purple in colour. We made the assumption that purple pixels in close proximity (up to 0.60 m away) to the predicted RS unit locations belonged to clusters of floral units of *S. dioica* or *C. nigra* in May and July imagery, respectively. Classification training and verification pixels were purposively selected from within these floral clusters (Fig. 3). For some predicted RS unit locations, no pink/purple pixels were found in the vicinity. 3 *S. dioica* and 2 *C. nigra* RS unit clusters were consequently used for identifying the location of training pixels for each species, respectively and 3 *S. dioica* and 2 *C. nigra* RS unit clusters were used for identifying verification pixels for each species, respectively. See Supporting Methods 1 for a description of how *S. dioica* and *C. nigra* clusters were designated.

For hedgerows, none of the target flowering hedgerow species flowered synchronously. *Prunus spinosa* flowering at the time of acquisition of our March image had finished flowering by May when the second image was acquired and during which time *Crataegus monogyna* was flowering. Similarly, *C. monogyna* had finished flowering by the time of the July image acquisition, during which time *Rubus fruticosus* was flowering. As the floral units of each of these species are white or almost white and flower in dense clusters often several metres long or more, any white floral unit pixels within hedgerow sections in imagery from each acquisition date could safely be allocated to the appropriate species (see Fig. 4).

## 2.5. Image training and classification

We used the semi-automatic classification (SCP) plugin (Congedo, 2016) in QGIS version 3.4.15 (QGIS, 2020) for training an ML classifier and running the classification. We chose this platform as it is open

source and has all classification and accuracy assessment tools within one easy-to-use graphical user interface.

We started by training and classifying the 3 cm images for each month. Each target flowering plant species formed a classification category within the classifications for their respective months. For each month we also created an 'other' classification category which contained all features within the imagery that we were not interested in classifying individually, such as green vegetation, soil or branches.

Training data were gathered for each flowering plant species classification category by selecting pixels within the imagery that we knew belonged to the floral component of each species based on our ground-truth data (see Section 2.4 and the flow chart in Fig. 5). We initially purposively selected 'seed' pixels (up to 64 seed pixels for each species) which were distributed as widely as possible across the study area for each respective species. For example, there were four large patches of *Prunus spinosa* in the hedgerow that were used for gathering training pixels. 16 seed pixels were purposively selected from each of these four patches leading to a total of 64 *P. spinosa* seed pixels. On the other hand, there was only one large patch of *Rubus fruticosus* used for gathering training data. All 64 *R. fruticosus* seed pixels were therefore purposively selected within this one patch.

We then used a region growing tool to select other pixels within a threshold distance (within 2000 digital numbers) of the seed pixel so that we ended up with groups of pixels at different training locations for each species, each with a spectral signature showing the mean digital number values in each band for that pixel group. We repeated the process for the 'other' classification category, making sure to select seed pixels across a range of different features so that we ended up with many sub-categories all contained under the main 'other' classification category. The classifications were later run at the level of this main 'other' category, e.g. if the algorithm allocated a pixel to a 'green vegetation'

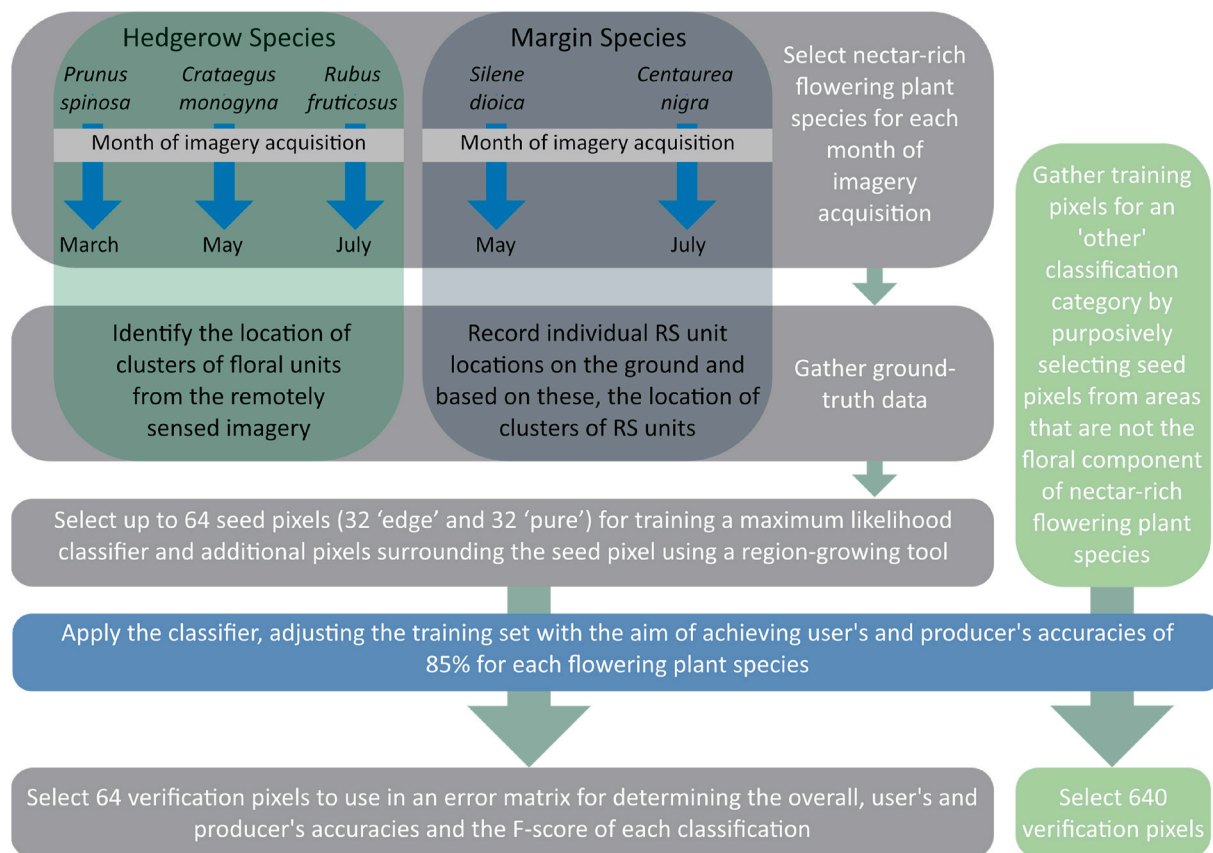


Fig. 5. Flow chart outlining the classification process for 3 cm imagery, from selecting nectar-rich flowering plant species to assessing the classification accuracy.

**Table 2**  
Number of verification pixels for each classification category included in the accuracy assessments for each month.

Month of data acquisition	Classification category	Number of verification pixels included in accuracy assessment	
		3 cm classifications	7 cm classifications
March	Other <sup>a</sup>	640	640
	<i>Prunus spinosa</i>	64	64
May	Other <sup>a</sup>	640	640
	<i>Silene dioica</i>	64	25
	<i>Crataegus monogyna</i>	64	64
July	Other <sup>a</sup>	640	640
	<i>Centaurea nigra</i>	64	25
	<i>Rubus fruticosus</i>	64	64

<sup>a</sup> Note that the 'other' category is a different set of pixels for each month.

sub-category, this would appear as belonging to the 'other' classification category in the classification output raster.

Pixels on the edge of clusters of floral units may contain other features as well, e.g. another flowering plant species or grass, which could affect the spectral signature within those edge pixels. We therefore chose both 'pure' and 'edge' seed pixels to cover spectral variability when gathering training data (up to 32 'pure' seed pixels and 32 'edge' seed pixels for each species). The former were the whitest/pinkest pixels (depending on flowering plant species) in the centre of patches. The latter were those pixels that were either on the edge of patches or, were in the centre of a very small patch and appeared to be mixed with other features. Supporting Table 2 provides the total number of training pixels for each classification category for each month (this total number includes the seed pixels and their nearby pixels selected using the region

growing tool).

ML classification algorithms were applied to the 3 cm imagery for each month using the training sets for each month, respectively. Several training set variants were applied to determine the influence upon classification accuracy, e.g. by including or excluding edge region training data. The aim of adjusting the training sets was to, where possible, obtain a minimum 85% for the user's and producer's accuracies for each nectar-rich flowering plant species classification category in the accuracy assessment process (see Supporting Table 2 and Section 2.6).

Spectral signatures for pixel groups created by the region growing tool within a particular classification category could be merged together to provide a mean spectral signature for the whole classification category, e.g. a merged signature for *Silene dioica*. If spectral signatures between different classification categories overlapped slightly, pixel groups could be removed from a classification category to change its mean spectral signature. This was a way of manually changing thresholds within a classification training set so that an image pixel would be allocated to one classification category over another.

Atmospheric conditions could potentially vary between the acquisition of 3 cm and 7 cm data for each month. This was unlikely however, as 3 cm and 7 cm data were acquired consecutively where possible (March and July 3 cm and 7 cm data were acquired consecutively on the same day, while May 3 cm and 7 cm data were acquired on consecutive days) and images were acquired under similar weather conditions (see Methods Section 2.2). As our target flowering plant species are very distinct colours, we hypothesised that 3 cm training data could also be used to classify 7 cm imagery (Dash et al., 2019). We therefore used training data collated for each month using 3 cm imagery to classify the 7 cm imagery for each month, respectively. Only the training set variants that resulted in the best classification accuracies for each month for 3 cm imagery were applied to the 7 cm imagery for each month.

We also verified whether 7 cm data were a high enough resolution to train a classification and achieve high classification accuracies. We subsequently created a training set using May 7 cm imagery, keeping the training pixel locations as similar as possible to those within the 3 cm imagery training set. We classified the May 7 cm image using this new training set.

### 2.6. Accuracy assessment

We carried out an independent accuracy assessment for each classification using error matrices, through which overall accuracy, user's accuracy and producer's accuracy metrics were calculated (as in Sankey et al., 2018; Schmidt et al., 2018), as well as an F-score (Inglada et al., 2015). The overall accuracy indicates the percentage of correctly classified pixels across the entire image (Strahler et al., 2006), using a subset of pixels for which ground-truth data are available (verification pixels). User's and producer's accuracies are a better indicator of how well an individual classification category has been classified. For X verification pixels classified as classification category a, user's accuracy tells us the percentage of those pixels that are actually classification category a on the ground (Strahler et al., 2006). For Y verification pixels that we know belong to a particular classification category b on the ground, producer's accuracy tells us the percentage of those pixels that have been correctly classified as category b (Strahler et al., 2006). The F-score combines both user's and producer's accuracies into a single metric (Inglada et al., 2015) using the following equation (Maxwell and Warner, 2020):  $F\text{-score} = (2 \times \text{user's accuracy} \times \text{producer's accuracy}) / (\text{user's accuracy} + \text{producer's accuracy})$ .

We also calculated a kappa statistic, which is an overall accuracy metric that accounts for pixels that may have been allocated to the correct classification category by chance (Congalton et al., 1983; Foody, 2020; Lillesand et al., 2015). The number of verification pixels used for each classification category can be found in Table 2. We aimed to select a minimum of 64 verification pixels for each flowering plant species as this was the maximum number of verification pixels we could obtain for *Silene dioica* when using 3 cm imagery and we kept the figure constant between species for 3 cm imagery. As we were unable to locate some of the floral unit clusters, we included 25 rather than the target 64 verification pixels for *S. dioica* and *C. nigra* in the May and July 7 cm classification accuracy assessments, respectively (Table 2). Full accuracy assessment methods and error matrices are provided in Supporting Methods 3 and Supporting Data 2, respectively.

Verification pixels included in the accuracy assessments were all at least 0.2 m away from pixels included within the training set or were

**Table 3**  
Highest overall classification accuracies and kappa statistics achieved in each month for 3 cm and 7 cm resolution imagery.

Classification	Overall Accuracy (%)		Kappa statistic	
	3 cm	7 cm	3 cm	7 cm
March	98.72	98.44	0.92	0.90
May	92.32	92.73	0.71	0.61
July	97.14	97.53	0.90	0.89

**Table 4**  
Producer's accuracies, user's accuracies and F-scores from the 3 cm and 7 cm classifications with best overall accuracy for each month.

Classification Month	Species	User's Accuracy (%)		Producer's Accuracy (%)		F-score	
		3 cm	7 cm	3 cm	7 cm	3 cm	7 cm
March	<i>Prunus spinosa</i>	98.25	98.18	87.5	84.38	0.93	0.91
May	<i>Silene dioica</i>	95.35	92.86	64.06	52.00	0.77	0.67
May	<i>Crataegus monogyna</i>	77.78	76.09	65.63	54.69	0.71	0.64
July	<i>Centaurea nigra</i>	91.80	86.96	87.50	80.00	0.90	0.83
July	<i>Rubus fruticosus</i>	91.04	92.06	95.31	90.63	0.93	0.91

very obviously in a different land-cover category, e.g. a training pixel clearly located in a section of gravel and the verification pixel clearly located in a section of grass. Given that imagery had only a 3 cm or 7 cm spatial resolution, 0.2 m was considered a sufficient distance to provide independence between training and accuracy data sets.

## 3. Results

### 3.1. Overall accuracy and kappa statistics

Error matrices constructed for each 3 cm resolution classification can be found in Supporting Data 2. Error matrices constructed for classifications carried out on 7 cm imagery can be found in Supporting Data 3. Note that only the classification training set variant for each month that achieved the greatest overall accuracy for 3 cm data was used for classifying the respective 7 cm imagery. The classification variants for each month and at each resolution that achieved the best overall classification accuracy using 3 cm data, are outlined in Table 3 along with their respective kappa statistic values.

In March, the training set for the initial 3 cm classification contained both pure and edge *Prunus spinosa* pixels. This resulted in an overall classification accuracy of 97.44%. The training set for a second 3 cm classification variant contained only pure *P. spinosa* pixels, resulting in the classification with the best overall accuracy (Table 3). The difference between the two was only 1.28%.

The May classification variant that resulted in the best overall accuracy also only used the pinkest *Silene dioica* pixels within the training set and excluded edge pixels. One variant was very poor (when using the pinkest *S. dioica* pixels only and, non-merged pixel group signatures for *S. dioica* and *Crataegus monogyna*), classifying all pixels as *C. monogyna*, resulting in a difference in overall accuracy of 83.98% between the most and least accurate classification variants. The July classification variant with the highest overall accuracy used the pure pixels for *Centaurea nigra* and *Rubus fruticosus* within the training set and not the edge pixels. Among the July classification variants, the lowest overall accuracy was 60.03%, a difference of 37.11% from the highest (See Supporting Data 2).

There was less than a 1% difference between overall accuracies for 3 cm and 7 cm classifications for each month, respectively, for all final classifications that used 3 cm training data. March 3 cm data resulted in higher overall accuracies than 7 cm data, but the reverse was true for May and July data. The difference between kappa statistics for March, May and July were 2%, 10% and 1%, respectively. The kappa statistic was higher for 3 cm resolution imagery for each month.

### 3.2. User's and producer's accuracies and F-scores

The user's and producer's accuracies and F-scores for each flowering plant species in their respective 3 cm and 7 cm classifications can be seen in Table 4. These were calculated from the classification variants that gave the best overall accuracy (Table 3). It should be noted that these classifications did not necessarily have the best user's and producer's accuracies for individual species. For example, one 3 cm classification variant resulted in a user's accuracy of 100.00% for *Centaurea nigra* as opposed to the 91.80% shown in Table 4. The producer's accuracy for

**Table 5**

Overall, producer's and user's accuracies and F-scores for nectar-rich flowering plant species in May 7 cm imagery when classified using the 7 cm training set.

Overall Accuracy (%)	Kappa statistic	User's Accuracy (%)		Producer's Accuracy (%)		F-score	
		<i>Silene dioica</i>	<i>Crataegus monogyna</i>	<i>Silene dioica</i>	<i>Crataegus monogyna</i>	<i>Silene dioica</i>	<i>Crataegus monogyna</i>
94.65	0.73	85.71	85.71	72.00	65.63	0.78	0.74

*C. nigra* in that 3 cm classification variant was only 26.56% (Supporting Data 2).

The difference between 3 cm and 7 cm classification user's accuracies for each species varied between 0.07% and 4.84%. User's accuracy was higher with 3 cm imagery for all species except *Rubus fruticosus*, where it was higher with 7 cm imagery. The difference between producer's accuracies for 3 cm and 7 cm imagery ranged between 3.12% and 12.06%. 3 cm data resulted in higher producer's accuracies in all cases. 3 cm data also resulted in higher F-scores for each species.

### 3.3. 7 cm training data

The results of the accuracy assessment for May when using training data collated from 7 cm imagery can be seen in Table 5 and, the error

matrix can be found in Supporting Data 4. The overall accuracy obtained for the 7 cm classification when training the classifier with 7 cm data was higher than both 3 cm and 7 cm classifications when trained with 3 cm data. The user's accuracy for *Silene dioica* was lower, but producer's accuracy was higher, for the 7 cm classification trained with 7 cm data than for both 3 cm and 7 cm classifications trained with 3 cm data. For *Crataegus monogyna*, user's accuracy for the 7 cm classification trained with 7 cm data was higher than both 3 cm and 7 cm classifications trained with 3 cm data. *C. monogyna* producer's accuracy was higher for the 7 cm classification trained with 7 cm data than that trained with 3 cm data, but the same as the 3 cm classification trained with 3 cm data. For both *S. dioica* and *C. monogyna*, the F-scores were higher for the classifications trained with 7 cm data than either the 3 cm and 7 cm classifications trained with 3 cm data.

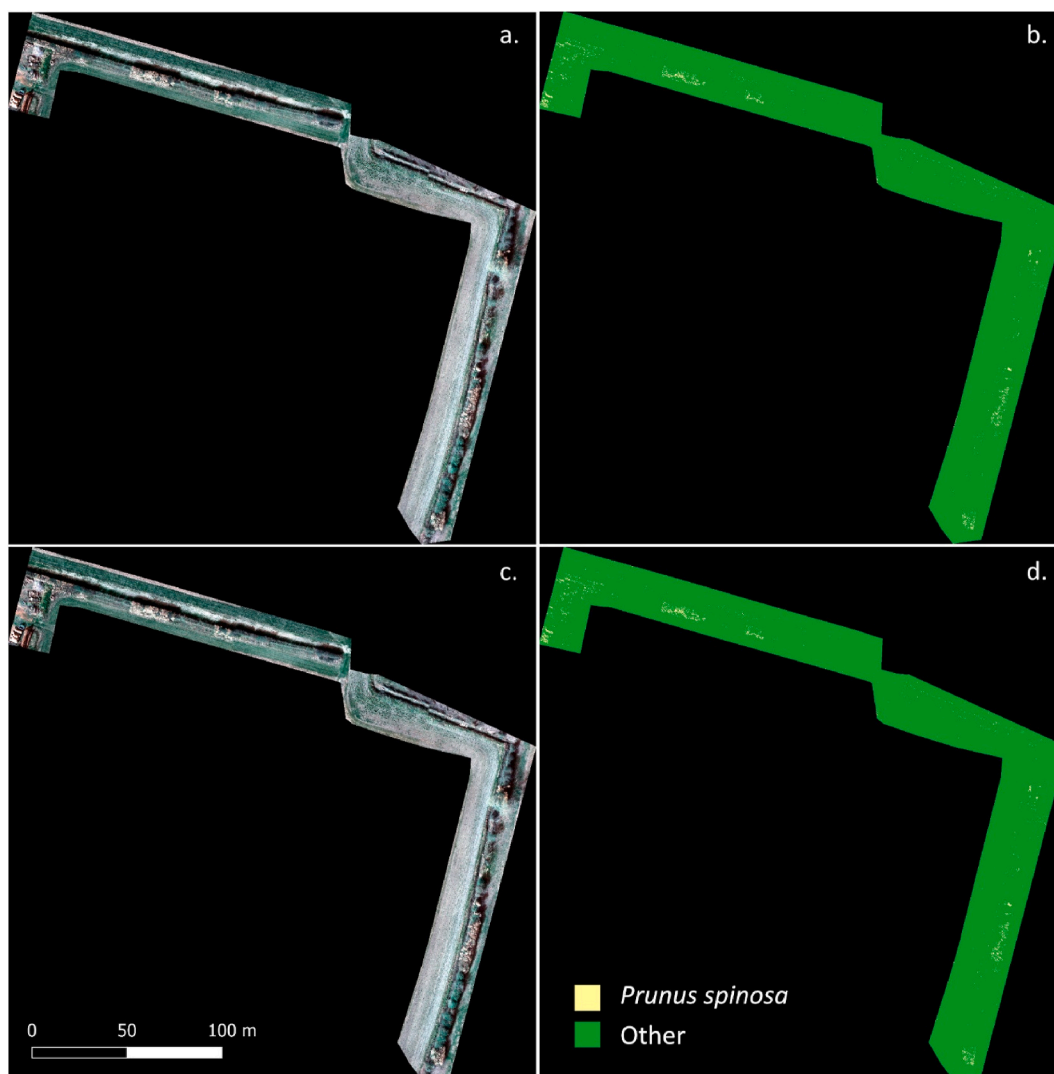


**Fig. 6.** a. The 3 cm image acquired of the study field in March. b. The 3 cm classification output for March with the best overall accuracy. c. The March 7 cm image acquired of the study field. d. The March 7 cm classification output.

## 4. Discussion

### 4.1. Suitability of 3 cm and 7 cm imagery for mapping nectar-rich flowering plant species

Our results indicate that multispectral aerial imagery can be used to classify individual flowering plant species with high nectar-value to pollinators (see Fig. 6 for an example classification of the whole area for March). For those classification variants that achieved the highest overall accuracies, these were well above the suggested target of 80–85% (e.g. see Foody, 2008 and Xavier et al., 2018). This is no surprise as the species under consideration had floral units with colours visibly distinct from the background vegetation (Dash et al., 2019). Kappa statistics were more variable, ranging between 0.61 for May 7 cm imagery and 0.92 for March 3 cm imagery. There is debate however, as to whether the kappa statistic is a useful metric for accuracy assessments (Bradter et al., 2020; Foody, 2020).

It was clear that 3 cm classification variants that excluded edge pixels within the training data for each month resulted in higher classification accuracies. This is likely because this reduces the spectral signature variability of pixels belonging to a particular flowering plant species category (Woodcock and Strahler, 1987). An alternative for dealing with mixed pixels in future studies could be to use a ‘fuzzy’ or ‘soft’ classification approach (e.g. see Foody and Arora, 1996; Shanmugam et al., 2006).

User’s and producer’s accuracies can be seen as more important for determining whether a particular flowering plant species has been correctly classified (Story and Congalton, 1986). For classifications with the best overall accuracy for each month and at each resolution, user’s and producer’s accuracies for *Prunus spinosa* and *Rubus fruticosus* were 80% or above. This is likely because although the floral units themselves are relatively small (Table 1), they flower in dense clusters within the hedgerow. Subsequently, there are likely to be fewer mixed pixels, which can reduce classification accuracies (Foody and Arora, 1996;

Shanmugam et al., 2006). *Crataegus monogyna* also consisted of small floral units forming dense clusters. User’s and producer’s accuracies of less than 80% for *C. monogyna* within classifications trained with 3 cm data were likely caused by spectral signature overlap with the synchronously flowering *Anthriscus sylvestris*, which can also flower in dense clusters (Fig. 7).

User’s and producer’s accuracies obtained for *Centaurea nigra* in July were also 80% or above at each resolution. Despite similar floral unit sizes to *C. nigra* (Table 1), *Silene dioica* had producer’s accuracies lower than 80% at each resolution, although the user’s accuracies were higher. A possible explanation for differences between the two species is that the leafy vegetation in May was not as long as in July. It is therefore possible that other features with similar spectral characteristics to *S. dioica*, such as branches in the hedgerow, were more exposed in May than in July (Fig. 8). Alternatively, many of the *S. dioica* floral units were positioned sideways rather than upright like the *C. nigra* units. This potentially meant that a smaller area of floral unit was seen from above, leading to pixels containing a greater proportion of other features. Although *S. dioica* floral units are bright pink, their sepals are dark purple, almost brown in colour. With the sideways positioning of *S. dioica* floral units and greater visibility of the sepals, it is possible that they were less spectrally distinguishable from other features such as branches when compared to *C. nigra*’s bright purple, upwardly-oriented floral units.

One way to address the misclassifications for both *C. monogyna* and *S. dioica* could be to combine spectral data with additional data such as vegetation height, for example through use of a decision tree (Sankey et al., 2018).

In each month the difference in overall accuracy between 3 cm and 7 cm imagery, when classified with 3 cm training data, was less than 1%. In May and July, the 7 cm classifications resulted in the higher accuracy. This suggests that the training data set prepared for the 3 cm imagery was suitable for applying to the 7 cm imagery. The 7 cm classification for May trained with 7 cm data resulted in an overall accuracy higher than both May classifications (3 cm and 7 cm) trained with 3 cm data. In line

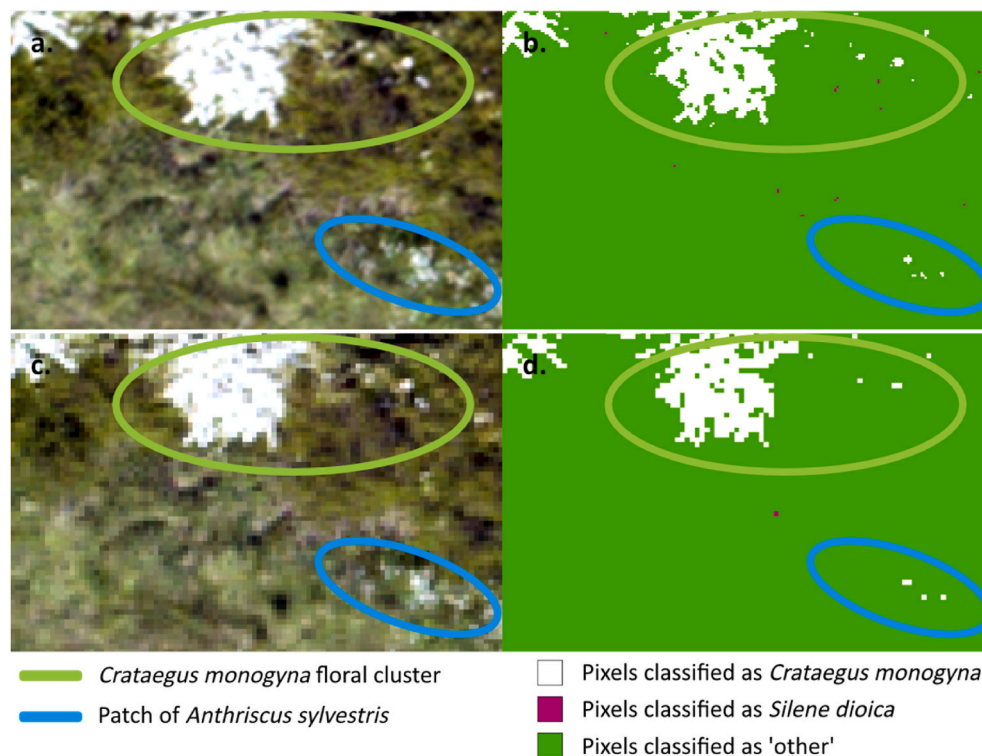
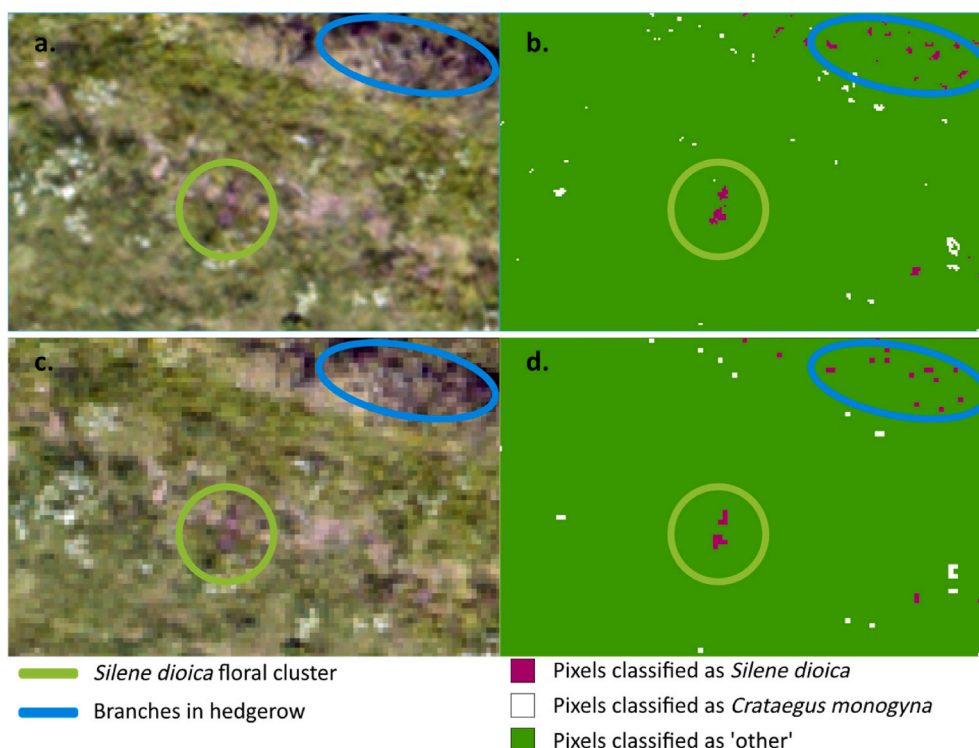


Fig. 7. a. Subsection of the original May 3 cm image with *Crataegus monogyna* and *Anthriscus sylvestris* circled. b. The 3 cm classification output with best overall accuracy showing pixels of *C. monogyna* correctly and incorrectly classified. c. Subsection of the original May 7 cm image. d. The 7 cm classification output showing pixels of *C. monogyna* correctly and incorrectly classified.



**Fig. 8.** a. Subsection of the original May 3 cm resolution image with *Silene dioica* and hedgerow branches circled. b. Subsection of the 3 cm classification output with the best overall accuracy showing pixels of *S. dioica* correctly and incorrectly classified. c. Subsection of the original May 7 cm image. d. The 7 cm classification output showing pixels of *S. dioica* correctly and incorrectly classified.

with other studies (Latty et al., 1985; Toll, 1985), this suggests that higher spatial resolution is not always necessary to achieve good classification accuracies. This is not surprising because, spectral variability within classification categories can increase with a spatial resolution that is too high and which therefore picks up greater detail. There is subsequently a higher likelihood of different features having overlapping spectral signatures (Pu et al., 2011; Gong and Howarth, 1990; Latty et al., 1985; Toll, 1985).

#### 4.2. Adapting the accuracy assessment process

In this study, verification pixels for use within the accuracy assessment process were selected in areas where we knew a particular species would not be growing. This is a similar approach to Holland and Aplin (2013), who only used accuracy assessment reference layer points that were linked to suitable ground-truth data. For example, we assumed that pixels in areas of hedgerow not belonging to focal flowering plant species, patches of shadow, short grass paths, the crop edge, etc. would constitute 'other' category pixels. Pixels classified as flowering plant species of interest, e.g. *Centaurea nigra*, in these areas were regarded as incorrect results.

These areas contained types of features that could potentially be confused with flowering plant species of interest, e.g. leafy vegetation, dry vegetation, patches of soil. We therefore believe that our study is a good initial test of whether our selected species' floral units can be detected using multispectral imagery.

However, for margin species, we did not establish control sections in the long-grass margins where we knew our focal species were absent. Other features in the margins that we had not accounted for could also be classified as our species of interest but would not be picked up within the accuracy assessment. Control areas containing species with potentially overlapping spectral signatures would be valuable in future studies, e.g. *Cirsium arvense* which in our study area was flowering synchronously to *C. nigra* albeit at a low abundance.

#### 4.3. Mapping floral resources and the implications for pollinator management

Many studies have differentiated between broad floral/vegetation categories or gradients of floral composition, with good degrees of success (e.g. see Xavier et al., 2018; Bradter et al., 2020; Feilhauer et al., 2013). Other studies have achieved high classification accuracies for individual plant species or species groups. When distinguishing between invasive *Pinus* species and native grassland vegetation for example, Dash et al. (2019) achieved kappa statistics higher than 0.996 when using cross-validation to verify different classification models.

Carl et al. (2017) used UAV imagery to estimate the number of *Robinia pseudoacacia* L. flowers per hectare in their study area: 5.3 million. Horton et al. (2017) successfully detected 84.3% of peach blossom pixels. With user's and producer's accuracies for *Rubus fruticosus*, *Centaurea nigra* and *Prunus spinosa* all above 80%, we achieved similar levels of accuracy for some species. To our knowledge, no others have attempted to use very high resolution remotely sensed imagery to map the floral cover of individual nectar-rich flowering plant species within arable field margins and hedgerows.

This is highly relevant for targeted pollinator management, as mapping the floral cover of nectar-rich flowering plant species would help identify gaps in the nectar-sugar supply. Resource gaps could subsequently be filled, helping to avoid the disconnect between nectar supply and pollinator demand at certain times of year, as identified by Jachula et al. (2021) and Timberlake et al. (2019). Timberlake et al. (2021) also demonstrated the importance of maintaining a continuous supply of nectar-rich flowering plant species across the pollinator foraging season. *Bombus terrestris* colony density was found to correlate with nectar provision in the late summer, highlighting the important role of nectar-rich flowering plant species such as *Hedera helix* at this time (Timberlake et al., 2021). *H. helix* is one of the 22 flowering plant species that together provide just over 90% of the British nectar sugar supply (Baude et al., 2016). In this study, we mapped the flowering plant

species that produced the greatest nectar sugar per floral unit in our study area during each image acquisition month. We included early and middle sections of the pollinator foraging season (see Sections 1.2 and 2.1). Extending our remote sensing methods to the top nectar producers that flower in the late summer/autumn, would be hugely beneficial for locating spatial gaps in the nectar supply at that time of year.

Remotely sensed data could be used when planning where to locate new nectar and pollen resources, taking into consideration different pollinator foraging ranges (Greenleaf et al., 2007; Knight et al., 2005). For example, data on the spatial availability of pollinator foraging resources could be combined with crop and yield information from precision agriculture tools, such as the Omnia™ tool provided by our industry partner Hutchinsons (2022). Farmers creating new pollinator-friendly habitats could locate it to fill spatial and temporal resource gaps for pollinators, while avoiding high-yielding areas of fields and within foraging range of specific pollinator-dependent crops, maximising benefits for both pollinators and farmers.

High resolution floral data could be used to improve our understanding of pollinator-habitat relationships. Remotely sensed imagery has already been used to determine the links between habitat structure and avian species (Fritz et al., 2018). High-resolution floral imagery could be fed into spatially-explicit models that estimate pollinator abundance or pollination service provision across a farmed landscape (Lonsdorf et al., 2009; Gardner et al., 2020 and others).

Tansey et al. (2009) suggest that fine scale remotely sensed data could be valuable to government bodies such as the UK Department for Environment, Food and Rural Affairs, for measuring and monitoring biodiversity within farmed landscapes. The implementation of agri-environment measures could be evaluated, in terms of their value to flower-visiting insects or their delivery of stated objectives related to floral resources (Tansey et al., 2009). Assessing the implementation of agri-environment measures is particularly relevant, given the current shift away from process-based to results-based agri-environment payments (Chaplin et al., 2021). This would be subject to the transferability of ground-truth data into an accurate map of resources for a wider range of nectar-rich flowering species, as discussed in Section 4.4. These data could also be useful for farmers/land-managers, to determine whether they are meeting agri-environment requirements. As many systems already employ remote sensing for monitoring crops (Daponte et al., 2019; Norasma et al., 2019; Tenkorang and Lowenberg-DoBoer, 2008), these practices could be extended to cover hedgerows and field margins and assess the resources available to pollinators.

#### 4.4. Future research requirements

In this study, we have established the potential for five key nectar-rich flowering plant species to be mapped at a single farm location, with varying accuracies. Determining whether additional flowering plant species can be reliably and accurately mapped is an important area of future research. Baude et al. (2016) list 22 flowering plant species as the top nectar-producers in Great Britain, contributing more than 90% of the annual nectar sugar supply. The prototype approach we present here could be extended to these 22 species, as a starting point for determining the viability of using high-resolution remote sensing for assessing the spatial and temporal distribution of the overall nectar sugar supply in British agricultural landscapes. However, we recommend for future studies using 7 cm imagery, that the number of floral units mapped on the ground be doubled to a minimum of approximately 200 floral units for species such as *Silene dioica* and *Centaurea nigra*, which have floral units of only several cm in width. This would provide a buffer should it not be possible to locate some of the floral units within the imagery, as was the case with our data.

Scaling up this research to test the classification accuracy of nectar-rich flowering plant species at multiple locations across different agricultural landscapes could potentially lead to the development of a spectral library of nectar-rich floral resources (Zhang et al., 2020). This

could be used by land managers and other stakeholders to map resources for pollinators across farming systems, without needing to re-train a classification. Constructing such a spectral library would require converting digital number values to reflectance values, as well as a detailed understanding of how the classification accuracy of nectar-rich floral resources is influenced by site conditions such as soil type (Gholizadeh et al., 2018; Pottier et al., 2014) and differing non-target background vegetation (Gebhardt et al., 2006). The vegetation composition in an agricultural system is itself connected to a number of factors such as management (Pywell et al., 2011) or environmental conditions such as soil water content (Critchley et al., 2006). An integral next step for this research is therefore to determine whether a key set of nectar-rich plant species of importance to pollinators, can be classified with similar accuracies to those obtained through this study across a range of farm systems with different environmental conditions and employing various management practices.

We have demonstrated the accuracy with which floral unit pixels of different nectar-rich plant species can be classified. We do not yet know the number of individual floral units each pixel represents on the ground. Estimates of floral unit density would be required for remotely sensed maps of floral resources to be translated directly into nectar sugar supply rates and this is an important area for future work. The work of Xavier et al. (2018) gives us confidence that this will be possible, at least for plant species with high enough user's/producer's accuracies. While not distinguishing between flower species, Xavier et al. (2018) found that the total floral cover as measured through drone surveys ( $m^2$ ) was positively correlated with the number of flowers on the ground. Pollinator visits were also positively correlated with both UAV-calculated floral cover and ground-based floral abundance data (Xavier et al., 2018).

If certain flowering plant species remain spectrally inseparable at the species level, they may still be separable into functional groups. Groups would have to be constructed based both on properties that make them spectrally distinguishable from another group, as well as those that make them attractive/accessible to pollinators, e.g. nectar sugar content (Kattenborn et al., 2019; Fornoff et al., 2017; Van Rijn and Wäckers, 2016).

Alternatively, for those species not separable with multispectral imagery, it could be worthwhile investigating the use of hyperspectral imagery (e.g. see Underwood et al., 2007; Kattenborn et al., 2019). Feilhauer et al. (2016) did not look at individual species, but demonstrated that plant pollination types (wind, insect or self-pollinating) could be distinguished and mapped using hyperspectral remote sensing. This was linked to the fact that they vary in canopy structure and leaf traits. For example, plants typically pollinated by insects tended to have a greater leaf area index compared to wind-pollinated species (Feilhauer et al., 2016). Using hyperspectral data does not always guarantee overall, user's and producer's accuracies higher than the 80–85% accuracy threshold widely accepted in the remote sensing literature (Foody, 2008; Xavier et al., 2018). When producing maps of white flowering and yellow flowering trees in Kenya, among other land use/land cover (LULC) classification categories, Abdel-Rahman et al. (2015) obtained overall accuracies of 88.15% and 83.67% when using hyperspectral data for February 2013 and January 2014, respectively. On the other hand, user's and producer's accuracies were below the 80–85% accuracy threshold for some of their LULC categories (Abdel-Rahman et al., 2015). With higher costs involved with hyperspectral data, it would be important to determine whether the additional cost is worth any increases in accuracy metrics obtained (Galbraith et al., 2015).

As noted in the introduction, we chose to use an ML classifier due to its ready availability (Lu and Weng, 2007) and its ease of use for applications on the ground, i.e. it is available through platforms such as the QGIS Semi-automatic Classification Plugin (SCP) (Congedo, 2016; QGIS, 2020). Nonetheless, with future studies it would be interesting to compare the performance of an ML classifier to a machine-learning

approach. This would be particularly valuable as freely available software with easy-to-use graphical user interfaces, such as the SCP QGIS plugin, have started to include machine-learning tools since the completion of this study (Congedo, 2021). Machine-learning approaches are non-parametric and therefore do not rely on normal distributions within data (Belgiu and Drăguț, 2016; Lu and Weng, 2007), nor do they require any prior understanding of how data relate to one another (Lary et al., 2016). They are also better able to deal with heterogeneity within classification categories (Grinand et al., 2013).

## 5. Conclusions

We demonstrate that five nectar-rich pollinator foraging resources can be mapped using multispectral data with very high spatial resolutions of 3–7 cm. Regardless of month of data acquisition and spatial resolution, overall accuracies are all high, ranging from 92.32% to 98.72%. Producer's and user's accuracies and F-scores for individual species are more variable. High classification accuracies are achieved for some species such as *Prunus spinosa* (98.25% user's accuracy and 87.50% producer's accuracy for 3 cm classifications). Lower accuracies are associated with species flowering concurrently to other flowering species with similar spectral properties or, at times of year when non-vegetation features with similar spectral properties such as branches are more exposed. Questions remain in terms of improving these lower user's and producer's accuracies. Nonetheless, we have provided a foundation upon which to build this work. Remotely sensing floral and other habitat resources will be increasingly valuable into the future as one of many management tools that can help prevent further pollinator declines.

## Data accessibility

All data have been deposited with the Natural Environment Research Council's (NERC) Environmental Information Data Centre (EIDC) (Barnsley et al., 2021).

## Author contributions

Sarah Barnsley performed the majority of fieldwork and analysis for this paper. Co-authors Dr Lynn V. Dicks and Professor Andrew A. Lovett helped to conceive the ideas and provided advice on fieldwork and on the use of GIS and remote-sensing platforms. Sarah Barnsley drafted the manuscript and Lynn V. Dicks and Andrew A. Lovett reviewed and edited the manuscript.

## Declaration of competing interest

The authors declare the following financial interests/personal relationships which may be considered as potential competing interests: PhD is part funded by industry partner H L Hutchinsons Ltd.

## Acknowledgements and Funding

We would like to thank the Natural Environment Research Council (grant codes NE/N014472/1 & 2, Studentship 1928670) and H L Hutchinsons Ltd. for funding this project as the iCASE partner to the Studentship. Many thanks go also to Spectrum Aviation for significant help with obtaining and processing the aerial imagery. We are grateful for the time and resources provided by Andrew and William Pitts and for their allowing us to use their farm as a base for this research. Thanks to the field store at University of East Anglia for loaning equipment.

## Appendix A. Supplementary data

Supplementary data to this article can be found online at <https://doi.org/10.1016/j.jenvman.2022.114942>.

## References

- Abdel-Rahman, E.M., Makori, D.M., Landmann, T., Piironen, R., Gasim, S., Pellikka, P., Raina, S.K., 2015. The Utility of AISA Eagle Hyperspectral Data and Random Forest Classifier for Flower Mapping. *Remote Sensing*, pp. 13298–13318. <https://doi.org/10.3390/rs71013298>.
- Agisoft, 2019. Metashape – photogrammetric processing of digital images and 3D spatial data generation [online] Available at: <https://www.agisoft.com/>. (Accessed 12 June 2020).
- Barnsley, S.B., Lovett, A.A., Dicks, L.V., 2021. Multispectral Airborne Imagery and Associated Classifications, Training Data and Validation Data, for Mapping Nectar-Rich Floral Resources for Pollinators, Northamptonshire, UK 2020. NERC Environmental Information Data Centre. <https://doi.org/10.5285/cf68be0c-e969-4190-8ec6-abeedb51b42c>.
- Baude, M., Kunin, W.E., Memmott, J., 2015a. Nectar Sugar Values of Common British Plant Species [AgriLand]. NERC Environmental Information Data Centre. <https://doi.org/10.5285/69402002-1676-4de9-a04e-d17e827db93c>.
- Baude, M., Kunin, W.E., Memmott, J., 2015b. Flower Density Values of Common British Plant Species [AgriLand]. NERC Environmental Information Data Centre. <https://doi.org/10.5285/6c6d3844-e95a-4f84-a12e-65be4731e934>.
- Baude, M., Kunin, W.E., Boatman, N.D., Conyers, S., Davies, N., Gillespie, M.A.K., Morton, R.D., Smart, S.M., Memmott, J., 2016. Historical nectar assessment reveals the fall and rise of floral resources in Britain. *Nature* 530, 85–88. <https://doi.org/10.1038/nature16532>.
- Belgiu, M., Drăguț, L., 2016. Random forest in remote sensing: a review of applications and future directions. *ISPRS J. Photogrammetry Remote Sens.* 114, 24–31. <https://doi.org/10.1016/j.isprsjprs.2016.01.011>.
- Betbeder, J., Hubert-Moy, L., Burel, F., Corgne, S., Baudry, J., 2015. Assessing ecological habitat structure from local to landscape scales using synthetic aperture radar. *Ecol. Indic.* (52), 545–557. <https://doi.org/10.1016/j.ecolind.2014.11.009>.
- Bradter, U., O'Connell, J., Kunin, W.E., Boffey, C.W.H., Ellis, R.J., Benton, T.G., 2020. Classifying grass-dominated habitats from remotely sensed data: the influence of spectral resolution, acquisition time and the vegetation classification system on accuracy and thematic resolution. *Sci. Total Environ.* 711, 1–14. <https://doi.org/10.1016/j.scitotenv.2019.134584>.
- Carl, C., Landgraf, D., van der Maaten-Theunissen, M., Biber, P., Pretzsch, H., 2017. *Robinia pseudoacacia* L. Flower analyzed by using an unmanned aerial vehicle (UAV). *Rem. Sens.* 9 (11), 1–19. <https://doi.org/10.3390/rs9111091>.
- Carrié, R., Lopes, M., Ouin, A., Andrieu, E., 2018. Bee diversity in crop fields is influenced by remotely-sensed nesting resources in surrounding permanent grasslands. *Ecol. Indic.* 90, 606–614. <https://doi.org/10.1016/j.ecolind.2018.03.054>.
- Carvell, C., Meek, W.R., Pywell, R.F., Goulson, D., Nowakowski, M., 2007. Comparing the efficacy of agri-environment schemes to enhance bumble bee abundance and diversity on arable field margins. *J. Appl. Ecol.* 44 (1), 29–40. <https://doi.org/10.1111/j.1365-2664.2006.01249.x>.
- Carvell, C., Bourke, A.F.G., Dreier, S., Freeman, S.N., Hulmes, S., Jordan, W.C., Redhead, J.W., Sumner, S., Wang, J., Heard, M.S., 2017. Bumblebee family lineage survival is enhanced in high-quality landscapes. *Nature* 543 (7646), 547–549. <https://doi.org/10.1038/nature21709>.
- Chaplin, S.P., Mills, J., Chiswell, H., 2021. Developing payment-by-results approaches for agri-environment schemes: experience from an arable trial in England. *Land Use Pol.* 109, 1–12. <https://doi.org/10.1016/j.landusepol.2021.105698> (105698).
- Chen, J., Shen, M., Zhu, X., Tang, Y., 2009. Indicator of flower status derived from in situ hyperspectral measurement in an alpine meadow on the Tibetan Plateau. *Ecol. Indic.* 9, 818–823. <https://doi.org/10.1016/j.ecolind.2008.09.009>.
- Congalton, R.G., Odeh, R.G., Mead, R.A., 1983. Assessing landsat classification accuracy using discrete multivariate analysis statistical techniques. *Photogramm. Eng. Rem. Sens.* 49 (12), 1671–1678.
- Congedo, L., 2016. Semi-Automatic Classification Plugin. Place of publication, Publisher [computer program], Version 6.4.0.
- Congedo, L., 2021. 3.4.4.5.1 random forest classification. <https://semiautomaticclassificationmanual.readthedocs.io/de/latest/randomForestTab.html>. (Accessed 24 August 2021).
- Critchley, C.N.R., Fowbert, J.A., Sherwood, A.J., Pywell, R.F., 2006. Vegetation development of sown grass margins in arable fields under a countrywide agri-environment scheme. *Biol. Conserv.* 132 (1) <https://doi.org/10.1016/j.biocon.2006.03.007>.
- Daponte, P., De Vito, L., Glielmo, L., Iannelli, L., Luzzza, D., Picariello, F., Silano, G., 2019. A review on the use of drones for precision agriculture. In: *IOP Conference Series: Earth and Environmental Science*, vol. 275, pp. 1–10. <https://doi.org/10.1088/1755-1315/275/1/012022> (12022).
- Dash, J.P., Watt, M.S., Paul, T.S.H., Morgenroth, J., Pearce, G.D., 2019. Early detection of invasive exotic trees using UAV and manned aircraft multispectral and LiDAR data. *Rem. Sens.* 11 (15), 1–21. <https://doi.org/10.3390/rs11151812>.
- Dicks, L.V., Baude, M., Roberts, S.P.M., Phillips, J., Green, M., Carvell, C., 2015. How much flower-rich habitat is enough for wild pollinators? Answering a key policy question with incomplete knowledge. *Ecol. Entomol.* 40 (S1), 22–35. <https://doi.org/10.1111/een.12226>.
- Dicks, L.V., Breeze, T.D., Ngo, H.T., Senapathi, D., An, J., Aizen, M.A., Basu, P., Buchori, D., Galetto, L., Garibaldi, L.A., Gemmill-Herren, B., Howlett, B.G., Imperatriz-Fonseca, V.L., Johnson, S.D., Kovács-Hostyánszki, A., Kwon, Y.J., Lattorff, H.M.G., Lungharwo, T., Seymour, C.L., Vanbergen, A.J., Potts, S.G., 2021. A global-scale expert assessment of drivers and risks associated with pollinator decline. *Nat. Ecol. Evol.* 5, 1453–1461. <https://doi.org/10.1038/s41559-021-01534-9>.

- Dixon, D.J., Callow, J.N., Duncan, J.M.A., Setterfield, S.A., Pauli, N., 2021. Satellite prediction of forest flowering phenology. *Rem. Sens. Environ.* 255, 1–13. <https://doi.org/10.1016/j.rse.2020.112197> (112197).
- Emorsgate Seeds, 2021. EM1 – basic general purpose meadow mixture. <https://wildseed.co.uk/mixtures/view/2>. (Accessed 23 July 2021).
- Feilhauer, H., Thonfeld, F., Faude, U., He, K.S., Rocchini, D., Schmidtlein, S., 2013. Assessing floristic composition with multispectral sensors – a comparison based on monotemporal and multiseasonal field spectra. *Int. J. Appl. Earth Obs. Geoinf.* 21, 218–229. <https://doi.org/10.1016/j.jag.2012.09.002>.
- Feilhauer, H., Doktor, D., Schmidtlein, S., Skidmore, A.K., 2016. Mapping pollination types with remote sensing. *J. Veg. Sci.* 27, 999–1011. <https://doi.org/10.1111/jvs.12421>.
- Fisher, J.R.B., Acosta, E.A., Denny-Frank, P.J., Kroeger, T., Boucher, T.M., 2018. Impact of satellite imagery spatial resolution on land use classification accuracy and modeled water quality. *Rem. Sens. Ecol. Conserv.* 4 (2), 137–149. <https://doi.org/10.1002/rse2.61>.
- Foody, G.M., 2008. Harshness in image classification accuracy assessment. *Int. J. Rem. Sens.* 29 (11), 3137–3158. <https://doi.org/10.1080/01431160701442120>.
- Foody, G.M., 2020. Explaining the unsuitability of the kappa coefficient in the assessment and comparison of the accuracy of thematic maps obtained by image classification. *Rem. Sens. Environ.* 239, 1–11. <https://doi.org/10.1016/j.rse.2019.111630>.
- Foody, G.M., Arora, M.K., 1996. Incorporating mixed pixels in the training, allocation and testing stages of supervised classifications. *Pattern Recogn. Lett.* 17 (13), 1389–1398. [https://doi.org/10.1016/S0167-8655\(96\)00095-5](https://doi.org/10.1016/S0167-8655(96)00095-5).
- Fornoff, F., Klein, A.-M., Hartig, F., Benadi, G., Venjakob, C., Schaefer, H.M., Ebeling, A., 2017. Functional flower traits and their diversity drive pollinator visitation. *Oikos* 126 (7), 1020–1030. <https://doi.org/10.1111/oik.03869>.
- Fritz, A., Li, L., Storch, I., Koch, B., 2018. UAV-derived habitat predictors contribute strongly to understanding avian species–habitat relationships on the Eastern Qinghai-Tibetan Plateau. *Rem. Sens. Ecol. Conserv.* 4 (1), 53–65. <https://doi.org/10.1002/rse2.73>.
- Galbraith, S.M., Vierling, L.A., Bosque-Pérez, N.A., 2015. Remote sensing and ecosystem services: current status and future opportunities for the study of bees and pollination-related services. *Curr. Fores. Rep.* 1, 261–274. <https://doi.org/10.1007/s40725-015-0024-6>.
- Gardner, E., Breeze, T.D., Clough, Y., Smith, H.G., Baldock, K.C.R., Campbell, A., Garratt, M.P.D., Gillespie, M.A.K., Kunin, W.E., McKerchar, M., Memmott, J., Potts, S.G., Senapathi, D., Stone, G.N., Wäckers, F., Westbury, D.B., Wilby, A., Oliver, T.H., 2020. Reliably predicting pollinator abundance: challenges of calibrating process-based ecological models. *Method. Ecol. Evol.* 11 (12), 1673–1689. <https://doi.org/10.1111/2041-210X.13483>.
- Garratt, M.P.D., Senapathi, D., Coston, D.J., Mortimer, S.R., Potts, S.G., 2017. The benefits of hedgerows for pollinators and natural enemies depends on hedge quality and landscape context. *Agric. Ecosyst. Environ.* 247, 363–370. <https://doi.org/10.1016/j.agee.2017.06.048>.
- Gebhardt, S., Schellberg, J., Lock, R., Kühbauch, W., 2006. Identification of broad-leaved dock (*Rumex obtusifolius* L.) on grassland by means of digital image processing. *Precis. Agric.* 7, 165–178. <https://doi.org/10.1007/s11119-006-9006-9>.
- Gholizadeh, A., Zizala, D., Saberioon, M., Borůvka, L., 2018. Soil organic carbon and texture retrieving and mapping using proximal, airborne and Sentinel-2 spectral imaging. *Rem. Sens. Environ.* 218, 89–103. <https://doi.org/10.1016/j.rse.2018.09.015>.
- Gong, P., Howarth, P.J., 1990. The use of structural information for improving land-cover classification accuracies at the rural-urban fringe. *Photogramm. Eng. Rem. Sens.* 56 (1), 67–73. DOI: 0099-1112/90/5601-67\$02.25/0.
- Goulson, D., Nicholls, E., Botías, C., Rotheray, E.L., 2015. Bee declines driven by combined stress from parasites, pesticides, and lack of flowers. *Science* 347 (6229), 1–9. <https://doi.org/10.1126/science.1255957>.
- Greenleaf, S.S., Williams, N.M., Winfree, R., Kremen, C., 2007. Bee foraging ranges and their relationship to body size. *Oecologia* 153, 589–596. <https://doi.org/10.1007/s00442-007-0752-9>.
- Grinand, C., Rakotomalala, F., Gond, V., Vaudry, R., Bernoux, M., Vieilledent, G., 2013. Estimating deforestation in tropical humid and dry forests in Madagascar from 2000 to 2010 using multi-date Landsat satellite images and the random forests classifier. *Rem. Sens. Environ.* 139, 68–80. <https://doi.org/10.1016/j.rse.2013.07.008>.
- Guo, M., Li, J., Sheng, C., Xu, J., Wu, L., 2017. A review of wetland remote sensing. *Sensors* 17 (4). <https://doi.org/10.3390/s17040777>.
- Häussler, J., Sahlín, U., Baey, C., Smith, H.G., Clough, Y., 2017. Pollinator population size and pollination ecosystem service responses to enhancing floral and nesting resources. *Ecol. Evol.* 7 (6), 1898–1908. <https://doi.org/10.1002/ece3.2765>.
- Holl, K., 1995. Nectar resources and their influence on butterfly communities on reclaimed coal surface mines. *Restor. Ecol.* 3 (2), 76–85. <https://doi.org/10.1111/j.1526-100X.1995.tb00080.x>.
- Holland, J., Aplin, P., 2013. Super-resolution image analysis as a means of monitoring bracken (*Pteridium aquilinum*) distributions. *ISPRS J. Photogrammetry Remote Sens.* 75, 48–63. <https://doi.org/10.1016/j.isprsjrs.2012.10.002>.
- Horton, R., Cano, E., Bulanon, D., Fallahi, E., 2017. Peach flower monitoring using aerial multispectral imaging. *J. Imag.* 3 (1), 1–10. <https://doi.org/10.3390/jimaging3010002>.
- Hutchinsons, 2021. Hutchinsons crop production specialists. <https://www.hhltd.co.uk>. (Accessed 23 July 2021).
- Hutchinsons, 2022. Omnia precision agronomy. <https://www.hhltd.co.uk/wp-content/uploads/2021/06/3397-Omnia-Brochure-Hutchinsons.pdf>. (Accessed 28 February 2022).
- Inglada, J., Arias, M., Tardy, B., Hagolle, O., Valero, S., Morin, D., Dedieu, G., Sepulcre, G., Bontemps, S., Defourny, P., Koetz, B., 2015. Assessment of an operational system for crop type map production using high temporal and spatial resolution satellite optical imagery. *Rem. Sens.* 7 (9), 12356–12379. <https://doi.org/10.3390/rs70912356>.
- Islam, K., Jashimuddin, M., Nath, B., Nath, T.K., 2018. Land use classification and change detection by using multi-temporal remotely sensed imagery: the case of Chhunati wildlife sanctuary, Bangladesh. *Egypt. J. Rem. Sens. Space Sci.* 21 (1), 37–47. <https://doi.org/10.1016/j.ejrs.2016.12.005>.
- Jachula, J., Denisow, B., Wrzesień, M., 2021. Habitat heterogeneity helps to mitigate pollinator nectar sugar deficit and discontinuity in an agricultural landscape. *Sci. Total Environ.* 782 (146909), 1–14. <https://doi.org/10.1016/j.scitotenv.2021.146909>.
- Kattenborn, T., Fassnacht, F.E., Schmidtlein, S., 2019. Differentiating plant functional types using reflectance: which traits make the difference? *Rem. Sens. Ecol. Conserv.* 5 (1), 5–19. <https://doi.org/10.1002/rse2.86>.
- Kleijn, D., Winfree, R., Bartomeus, I., et al., 2015. Delivery of crop pollination services is an insufficient argument for wild pollinator conservation. *Nat. Commun.* 6 (7414), 1–8. <https://doi.org/10.1038/ncomms8414>.
- Knight, M.E., Martin, A.P., Bishop, S., Osborne, J.L., Hale, R.J., Sanderson, R.A., Goulson, D., 2005. An interspecific comparison of foraging range and nest density of four bumblebee (*Bombus*) species. *Mol. Ecol.* 14 (6), 1811–1820. <https://doi.org/10.1111/j.1365-294X.2005.02540.x>.
- Kos, T., Markežić, I., Pokrajčić, J., 2010. Effects of multipath reception on GPS positioning performance. In: *52nd International Symposium ELMAR-2010*, Zadar, Croatia, 15–17 September 2010. IEEE, pp. 399–402.
- Landmann, T., Feilhauer, H., Shen, M., Chen, J., Raina, S., 2018. Mapping the distribution and abundance of flowering plants using hyperspectral sensing. In: *Thenkabail, P.S., Lyon, J.G., Huete, A. (Eds.), Advanced Applications in Remote Sensing of Agricultural Crops and Natural Vegetation*. CRC Press, pp. 69–78.
- Langlois, A., Jacquemart, A.-L., Piqueray, J., 2020. Contribution of extensive farming practices to the supply of floral resources for pollinators. *Insects* 11 (818), 1–19. <https://doi.org/10.3390/insects11110818>.
- Lary, D.J., Alavi, A.H., Gandomi, A.H., Walker, A.L., 2016. Machine learning in geosciences and remote sensing. *Geosci. Front.* 7 (1), 3–10. <https://doi.org/10.1016/j.gsf.2015.07.003>.
- Latty, R.S., Nelson, R., Markham, B., Williams, D., Toll, D., Irons, J., 1985. Performance comparisons between information extraction techniques using variable spatial resolution data. *Photogramm. Eng. Rem. Sens.* 51 (9), 1459–1470. DOI: 0099-1112/85/5109-1459\$02.25/0.
- Lillesand, T.M., Kiefer, R.W., Chipman, J.W., 2015. *Remote Sensing and Image Interpretation*, seventh ed. Wiley, Hoboken.
- Lonsdorf, E., Kremen, C., Ricketts, T., Winfree, R., Williams, N., Greenleaf, S., 2009. Modelling pollination services across agricultural landscapes. *Ann. Bot.* 103 (9), 1589–1600. <https://doi.org/10.1093/aob/mcp069>.
- Lu, D., Weng, Q., 2007. A survey of image classification methods and techniques for improving classification performance. *Int. J. Rem. Sens.* 28 (5), 823–870. <https://doi.org/10.1080/01431160600746456>.
- Maxwell, A.E., Warner, T.A., 2020. Thematic classification accuracy assessment with inherently uncertain boundaries: an argument for center-weighted accuracy assessment metrics. *Rem. Sens.* 12, 1–21. <https://doi.org/10.3390/rs12121905> (1905).
- Mekik, C., Can, O., 2010. An investigation on multipath errors in real time kinematic GPS method. *Sci. Res. Essays* 5 (16), 2186–2200. <https://doi.org/10.5897/SRE.9000175>.
- Nature Gate, 2020. Plants. <http://www.luontoportti.com/suomi/en/kasvit/>. (Accessed 7 December 2020).
- Norasma, C.Y.N., Fadzilah, M.A., Roslin, N.A., Zanariah, Z.W.N., Tarmidi, Z., Candra, F. S., 2019. Unmanned aerial Vehicle applications in agriculture. In: *IOP Conference Series: Materials Science and Engineering*, vol. 506, pp. 1–10. <https://doi.org/10.1088/1757-899X/506/1/012063> (012063).
- Nowakowski, M., Pywell, R., 2016. *Habitat Creation and Management for Pollinators*. Centre for Ecology and Hydrology, Wallingford, UK.
- Ollerton, J., Erenler, H., Edwards, M., Crockett, R., 2014. Extinctions of aculeate pollinators in Britain and the role of large-scale agricultural changes. *Science* 346 (6215), 1360–1362. <https://doi.org/10.1126/science.1257259>.
- Ollerton, J., 2017. Pollinator diversity: distribution, ecological function, and conservation. *Annu. Rev. Ecol. Evol. Syst.* 48 (1), 353–376. <https://doi.org/10.1146/annurev-ecolsys-110316-022919>.
- Pettorelli, N., Schulte to Bühne, H., Tulloch, A., Dubois, G., Macinnis-Ng, C., Queirós, A. M., Keith, D.A., Wegmann, M., Schrodt, F., Stellmes, M., Sonnenschein, R., Geller, G. N., Roy, S., Somers, B., Murray, N., Bland, L., Geizendorfer, I., Kerr, J.T., Broszeit, S., Leitão, P.J., Duncan, C., El Serafy, G., He, K.S., Blanchard, J.L., Lucas, R., Mairota, P., Webb, T.J., Nicholson, E., 2018. Satellite remote sensing of ecosystem functions: opportunities, challenges and way forward. *Rem. Sens. Ecol. Conserv.* 4 (2), 71–93. <https://doi.org/10.1002/rse2.59>.
- Pottier, J., Malenovsky, Z., Psomas, A., Homolová, L., Schaeppman, M.E., Choler, P., Thuiller, W., Guisan, A., Zimmermann, N.E., 2014. Modelling plant species distribution in alpine grasslands using airborne imaging spectroscopy. *Biol. Lett.* 10 (7), 1–4. <https://doi.org/10.1098/rsbl.2014.0347>.
- Potts, S.G., Biesmeijer, J.C., Kremen, C., Neumann, P., Schweiger, O., Kunin, W.E., 2010. Global pollinator declines: trends, impacts and drivers. *Trends Ecol. Evol.* 25 (6), 345–353. <https://doi.org/10.1016/j.tree.2010.01.007>.
- Potts, S.G., Imperatriz-Fonseca, V., Ngo, H.T., Aizen, M.A., Biesmeijer, J.C., Breeze, T.D., Dicks, L.V., Garibaldi, L.A., Hill, R., Settele, J., Vanbergen, A.J., 2016. Safeguarding pollinators and their values to human well-being. *Nature* 540, 220–229. <https://doi.org/10.1038/nature20588>.

- Pu, R., Landry, S., Yu, Q., 2011. Object-based urban detailed land cover classification with high spatial resolution IKONOS imagery. *Int. J. Rem. Sens.* 32 (12), 3285–3308. <https://doi.org/10.1080/01431161003745657>.
- Pywell, R.F., Warman, E.A., Carvell, C., Sparks, T.H., Dicks, L.V., Bennett, D., Wright, A., Critchley, C.N.R., Sherwood, A., 2005. Providing foraging resources for bumblebees in intensively farmed landscapes. *Biol. Conserv.* 121 (4), 479–494. <https://doi.org/10.1016/j.biocon.2004.05.020>.
- Pywell, R.F., Meeke, W.R., Hulmes, L., Hulmes, S., James, K.L., Nowakowski, M., Carvell, C., 2011. Management to enhance pollen and nectar resources for bumblebees and butterflies within intensively farmed landscapes. *J. Insect Conserv.* 15, 853–864. <https://doi.org/10.1007/s10841-011-9383-x>.
- QGIS, 2020. QGIS Geographic Information System. Open Source Geospatial Foundation Project. Madeira [computer program], Version 3.4.15.
- Ricketts, T.H., Regetz, J., Steffan-Dewenter, I., Cunningham, S.A., Kremen, C., Bogdanski, A., Gemmill-Herren, B., Greenleaf, S.S., Klein, A.M., Mayfield, M.M., Morandin, L.A., Ochieng, A., Potts, S.G., Viana, B.F., 2008. Landscape effects on crop pollination services: are there general patterns? *Ecol. Lett.* 11 (5), 499–515. <https://doi.org/10.1111/j.1461-0248.2008.01157.x>.
- Sankey, T.T., McVay, J., Swetnam, T.L., McClaran, M.P., Heilman, P., Nichols, M., 2018. UAV hyperspectral and lidar data and their fusion for arid and semi-arid land vegetation monitoring. *Rem. Sens. Ecol. Conserv.* 4 (1), 20–33. <https://doi.org/10.1002/rse2.44>.
- Scheper, J., Holzschuh, A., Kuussaari, M., Potts, S.G., Rundlöf, M., Smith, H.G., Kleijn, D., 2013. Environmental factors driving the effectiveness of European agri-environmental measures in mitigating pollinator loss – a meta-analysis. *Ecol. Lett.* 16 (7), 912–920. <https://doi.org/10.1111/ele.12128>.
- Schmidt, J., Fassnacht, F.E., Förster, M., Schmidlein, S., 2018. Synergetic use of Sentinel-1 and Sentinel-2 for assessments of heathland conservation status. *Rem. Sens. Ecol. Conserv.* 4 (3), 225–239. <https://doi.org/10.1002/rse2.68>.
- Shanmugam, P., Ahn, Y.-H., Sanjeevi, S., 2006. A comparison of the classification of wetland characteristics by linear spectral mixture modelling and traditional hard classifiers on multispectral remotely sensed imagery in southern India. *Ecol. Model.* 194 (4), 379–394. <https://doi.org/10.1016/j.ecolmodel.2005.10.033>.
- Staley, J.T., Sparks, T.H., Croxton, P.J., Baldock, K.C.R., Heard, M.S., Hulmes, S., Hulmes, L., Peyton, J., Amy, S.R., Pywell, R.F., 2012. Long-term effects of hedgerow management policies on resource provision for wildlife. *Biol. Conserv.* 145 (1), 24–29. <https://doi.org/10.1016/j.biocon.2011.09.006>.
- Story, M., Congalton, R.G., 1986. Accuracy assessment: a user's perspective. *Photogramm. Eng. Rem. Sens.* 52 (3), 397–399. [0099-1112/86/5203-397\\$02.25/0](https://doi.org/10.1080/0099-1112/86/5203-397$02.25/0).
- Strahler, A.H., Boschetti, L., Foody, G.M., Friedl, M.A., Hansen, M.C., Herold, M., Mayaux, P., Morisette, J.T., Stehman, S.V., Woodcock, C.E., 2006. Global Land Cover Validation: Recommendations for Evaluation and Accuracy Assessment of Global Land Cover Maps. Italy: European Commission, Directorate-General Joint Research Centre, Institute for Environment and Sustainability.
- Tansey, K., Chambers, I., Anstee, A., Denniss, A., Lamb, A., 2009. Object-oriented classification of very high resolution airborne imagery for the extraction of hedgerows and field margin cover in agricultural areas. *Appl. Geogr.* 29 (2), 145–157. <https://doi.org/10.1016/j.apgeog.2008.08.004>.
- Tenkorang, F., Lowenberg-DoBoer, J., 2008. On-farm profitability of remote sensing in agriculture. *J. Terr. Obs.* 1 (1), 50–59.
- Timberlake, T.P., Vaughan, I.P., Memmott, J., 2019. Phenology of farmland floral resources reveals seasonal gaps in nectar availability for bumblebees. *J. Appl. Ecol.* 56 (7), 1585–1596. <https://doi.org/10.1111/1365-2664.13403>.
- Timberlake, T.P., Vaughan, I.P., Baude, M., Memmott, J., 2021. Bumblebee colony density on farmland is influenced by late-summer nectar supply and garden cover. *J. Appl. Ecol.* 1–11. <https://doi.org/10.1111/1365-2664.13826>, 00.
- Toll, D.L., 1985. Effect of landsat thematic mapper sensor parameters on land cover classification. *Rem. Sens. Environ.* 17 (2), 129–140. [https://doi.org/10.1016/0034-4257\(85\)90069-0](https://doi.org/10.1016/0034-4257(85)90069-0).
- Topcon, 2020. Hiper V. <https://www.topconpositioning.com/support/products/hiper-v>. (Accessed 1 December 2020).
- Underwood, E.C., Ustin, S.L., Ramirez, C.M., 2007. A Comparison of Spatial and Spectral Image Resolution for Mapping Invasive Plants in Coastal California, vol. 39. *Environmental Management*, pp. 63–83. <https://doi.org/10.1007/s00267-005-0228-9>.
- Vannier, C., Hubert-Moy, L., 2008. Detection of wooded hedgerows in high resolution satellite images using an object-oriented method. In: *IEEE International Geoscience and Remote Sensing Symposium 2008*, Boston, MA, USA, 7–11 July 2008. IEEE, pp. 731–734. <https://doi.org/10.1109/IGARSS.2008.4779826>.
- Vannier, C., Vasseur, C., Hubert-Moy, L., Baudry, J., 2011. Multiscale ecological assessment of remote sensing images. *Landsc. Ecol.* 26 (8), 1053–1069. <https://doi.org/10.1007/s10980-011-9626-y>.
- Van Rijn, P.C.J., Wäckers, F.L., 2016. Nectar accessibility determines fitness, flower choice and abundance of hoverflies that provide natural pest control. *J. Appl. Ecol.* 53 (3), 925–933. <https://doi.org/10.1111/1365-2664.12605>.
- Willcox, B.K., Robson, A.J., Howlett, B.G., Rader, R., 2018. Toward an integrated approach to crop production and pollination ecology through the application of remote sensing. *PeerJ* 6, e5806. <https://doi.org/10.7717/peerj.5806>.
- Willmer, P., 2011. *Pollination and Floral Ecology*. Princeton University Press, Princeton, New Jersey.
- Woodcock, C.E., Strahler, A.H., 1987. The factor of scale in remote sensing. *Rem. Sens. Environ.* 21 (3), 311–332. [https://doi.org/10.1016/0034-4257\(87\)90015-0](https://doi.org/10.1016/0034-4257(87)90015-0).
- Xavier, S.S., Coffin, A.W., Olson, D.M., Schmidt, J.M., 2018. Remotely estimating beneficial arthropod populations: implications of a low-cost small unmanned aerial system. *Rem. Sens.* 10 (9), 1485. <https://doi.org/10.3390/rs10091485>.
- Zhang, J., Wang, C., Yuan, L., Liu, P., Zhang, Y., Wu, K., 2020. Construction of a plant spectral library based on an optimised feature selection method. *Biosyst. Eng.* 195, 1–16. <https://doi.org/10.1016/j.biosystemseng.2020.04.008>.

## Further reading

- RTKLIB, 2013. RTKLIB: An Open Source Program Package for GNSS Positioning [computer program], Version 2.4.2.